SUPPLEMENTARY INFORMATION:

Kinetically assembled binary nanoparticle networks

Jiuling Wang, Brian Hyun-jong Lee, Gaurav Arya*

Department of Mechanical Engineering and Materials Science

Duke University, Durham, NC 27708, USA

1. Lattice model used for simulating assembly of a binary nanoparticle system

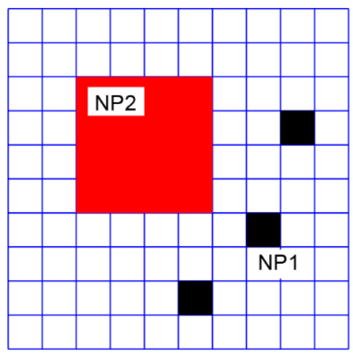

Fig. S1. Schematic showing large NPs (NP2) and small NPs (NP1) employed in our simulations. Large NPs shown in red occupy 4×4 lattice sites while small NPs shown in black occupy a single 1×1 lattice site.

2. Results obtained from assembly of a single nanoparticle species

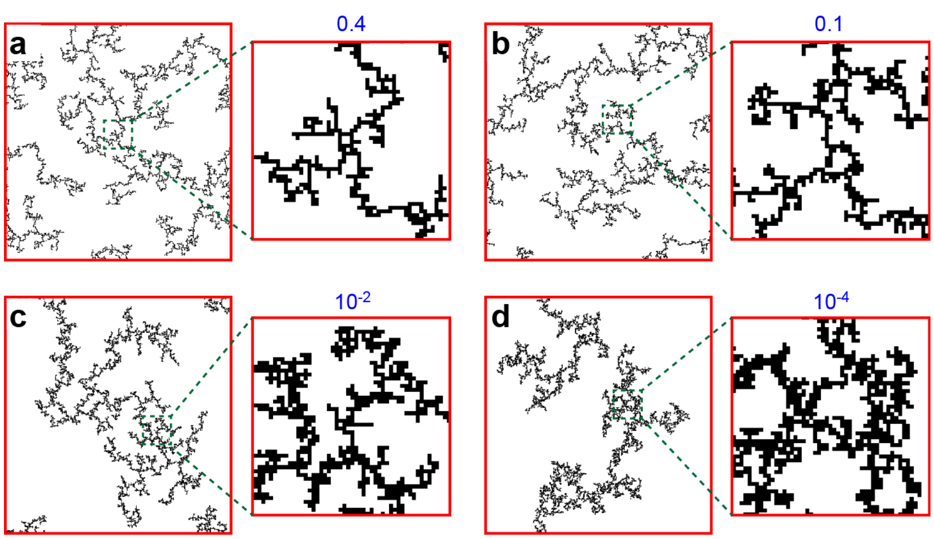

Fig. S2 Representative aggregates obtained from assembly of a single species of NPs with different sticking probabilities. The number of NPs are fixed at $N = 13{,}200$. The sticking probabilities are 0.4 (a), 0.1 (b), 10^{-2} (c), and 10^{-4} (d), as specified in each figure.

3. Kinetics of nanoparticles (NPs) assembly

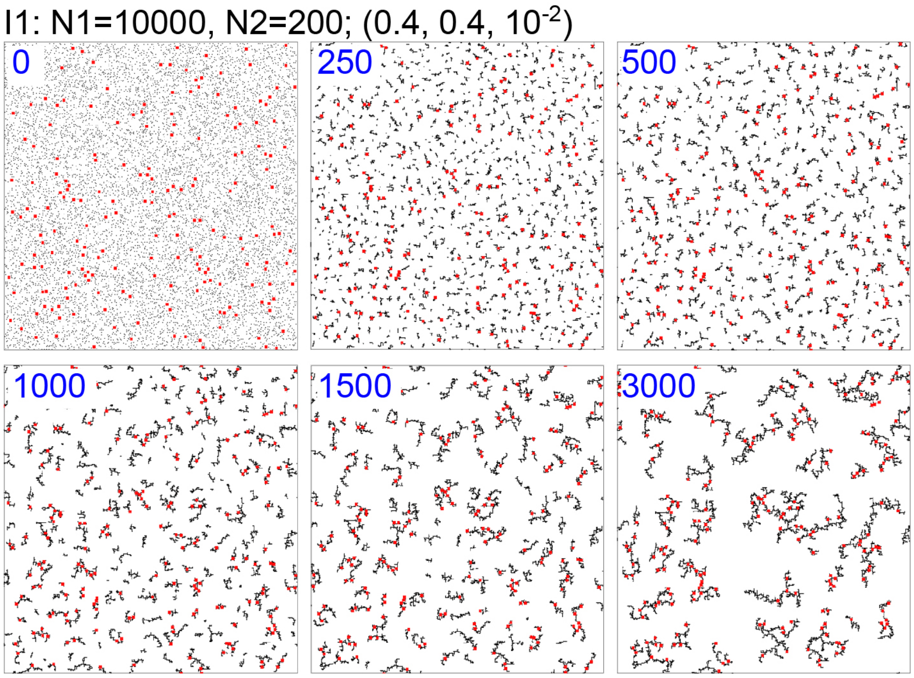

Fig. S3 Representative snapshots showing the kinetics of NPs assembly when N_1=10000, N_2=200, p_{11}=0.4, p_{12}=0.4 and p_{22}=10^{-2}. The numbers in blue are the corresponding simulation time steps.

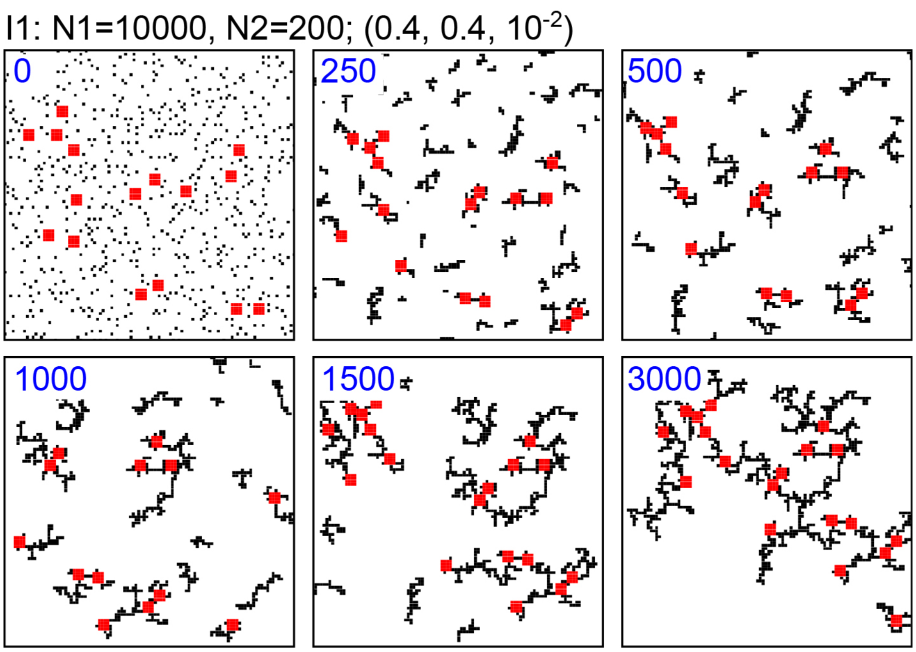

Fig. S4 Closeups of representative snapshots showed in Fig. S1.

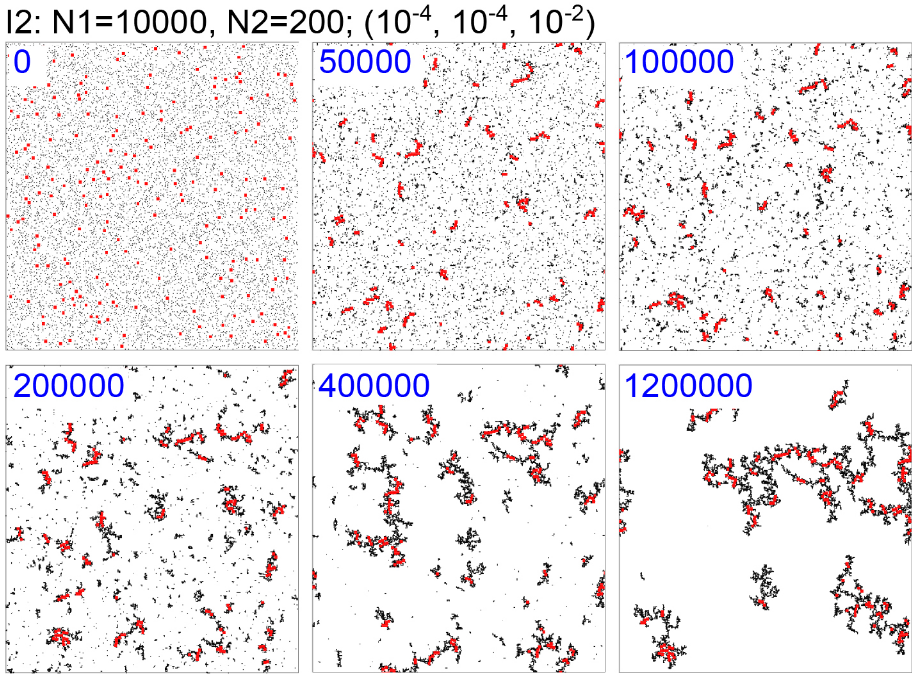

Fig. S5 Representative snapshots showing the kinetics of NPs assembly when N_1=10000, N_2=200, $p_{11}=10^{-4}$, $p_{12}=10^{-4}$ and $p_{22}=10^{-2}$.

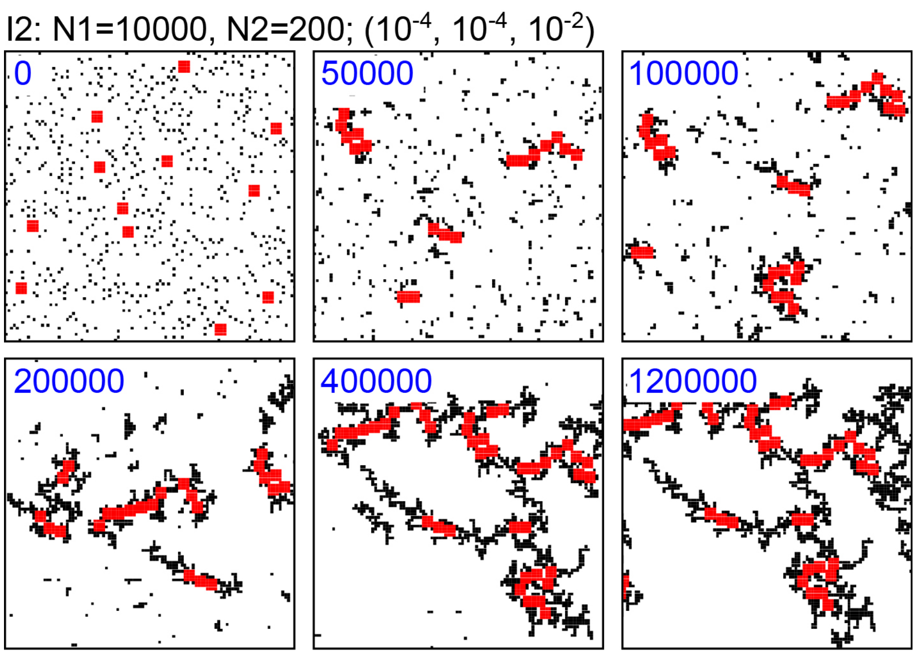

Fig. S6 Closeups of representative snapshots showed in Fig. S3.

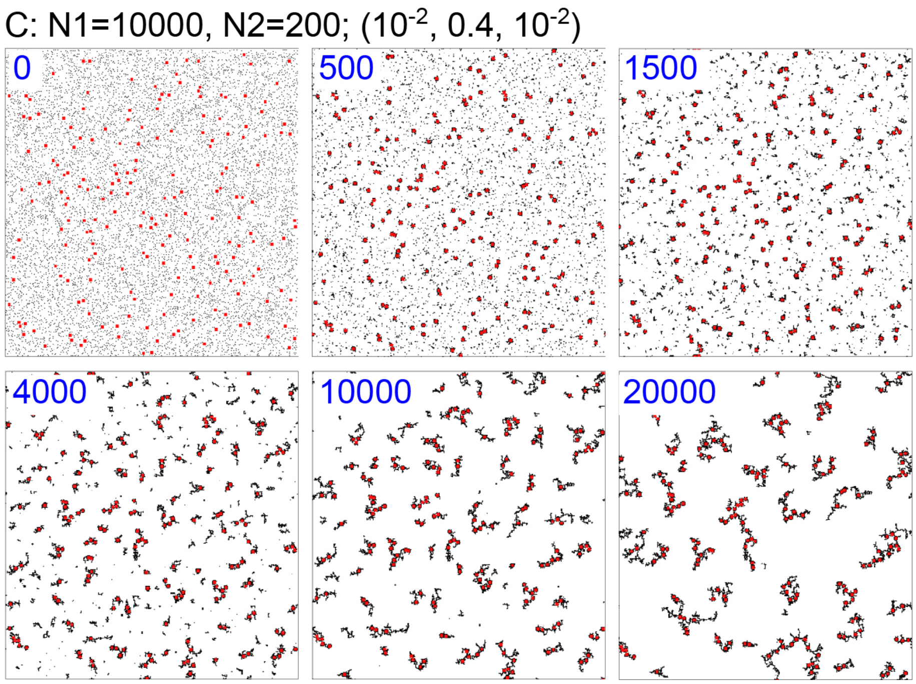

Fig. S7 Representative snapshots showing the kinetics of NPs assembly when N_1=10000, N_2=200, $p_{11}=10^{-2}$, p_{12}=0.4 and $p_{22}=10^{-2}$.

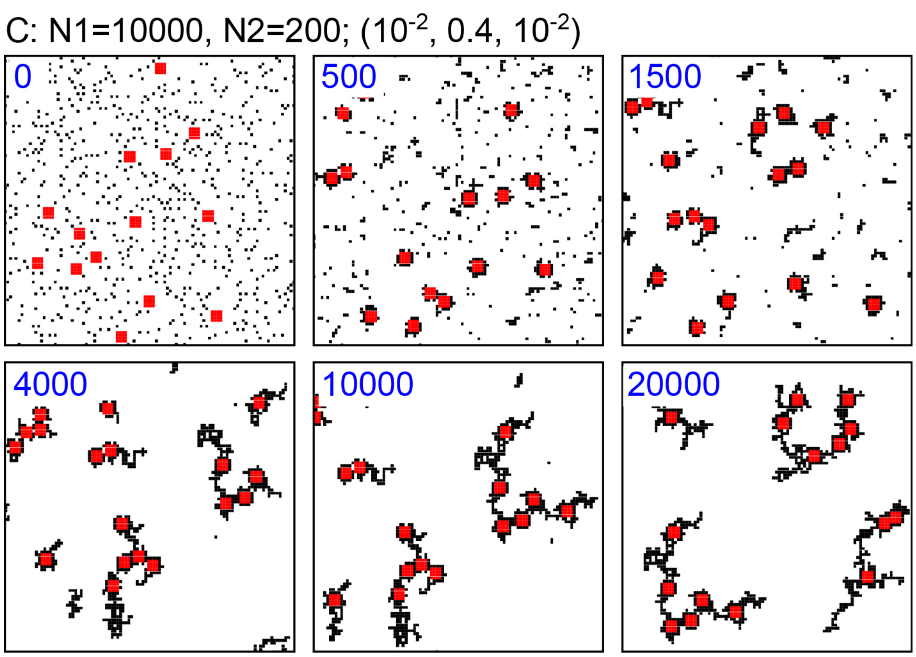

Fig. S8 Closeups of representative snapshots showed in Fig. S5.

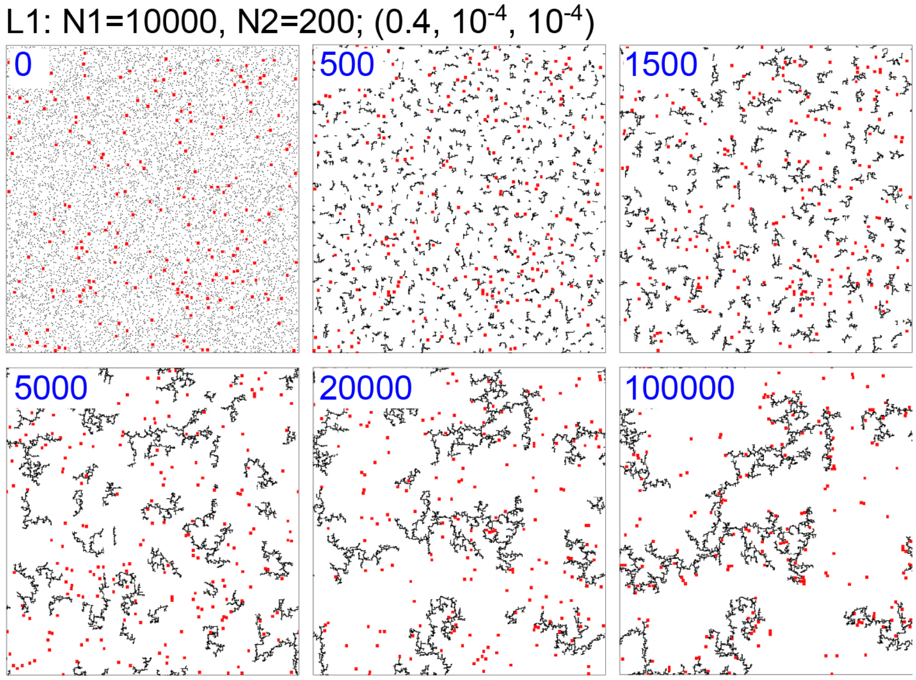

Fig. S9 Representative snapshots showing the kinetics of NPs assembly when N_1=10000, N_2=200, p_{11}=0.4, $p_{12}=10^{-4}$ and $p_{22}=10^{-4}$.

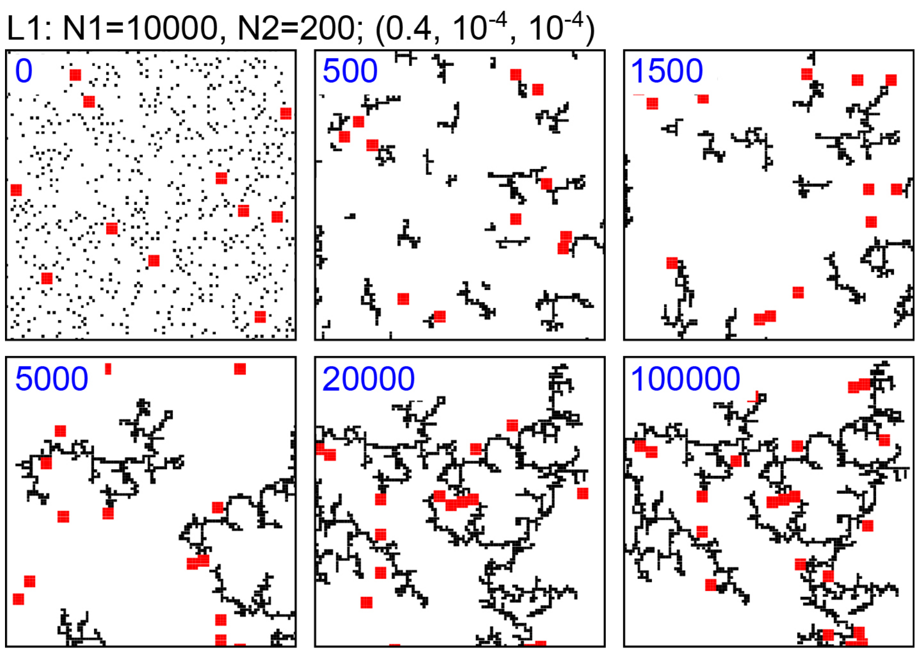

Fig. S10 Closeups of representative snapshots showed in Fig. S7.

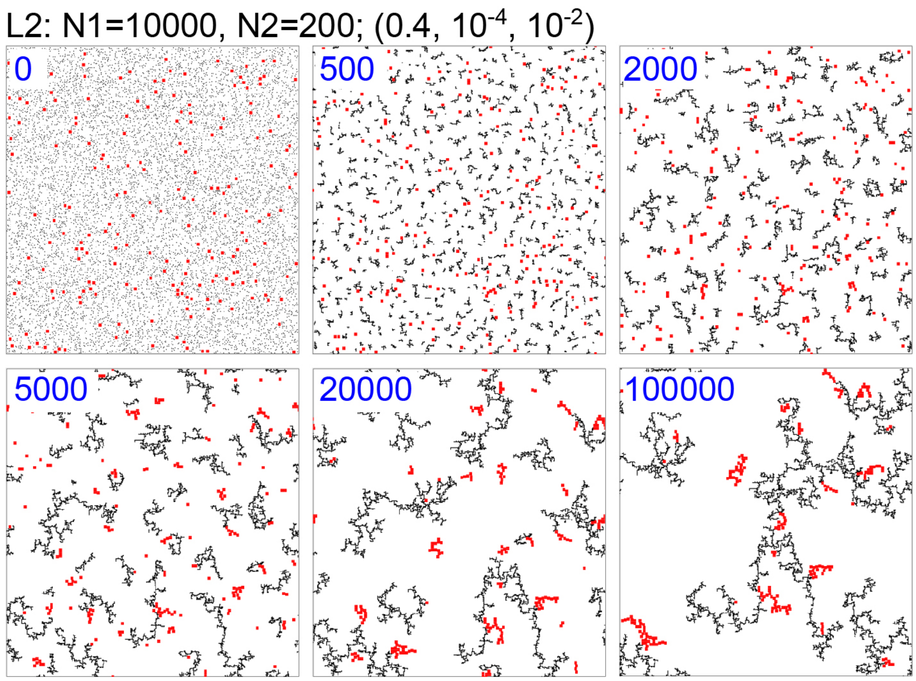

Fig. S11 Representative snapshots showing the kinetics of NPs assembly when N_1=10000, N_2=200, p_{11}=0.4, $p_{12}=10^{-4}$ and $p_{22}=10^{-2}$.

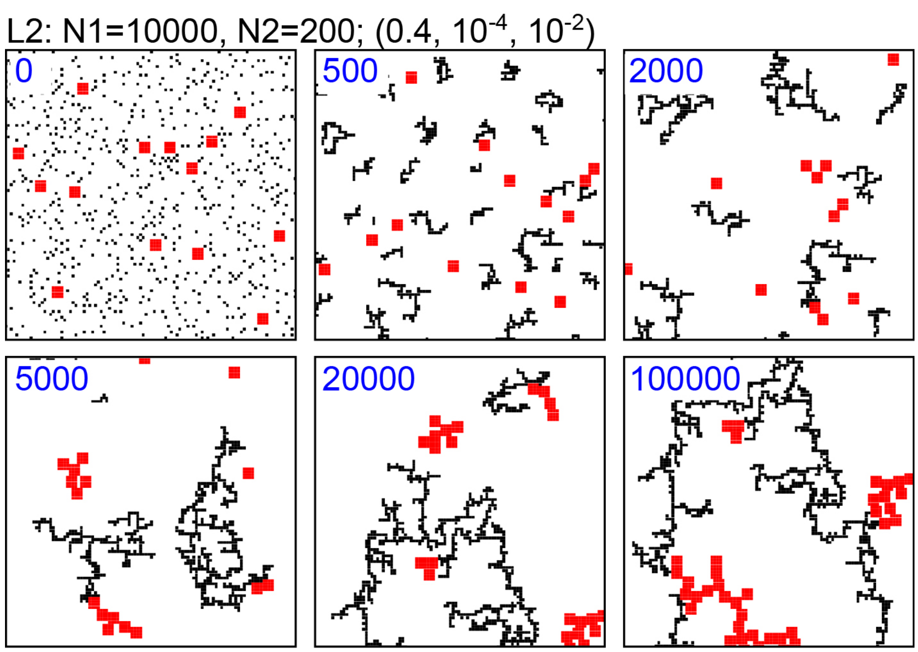

Fig. S12 Closeups of representative snapshots showed in Fig. S9.

4. Local composition of the structures

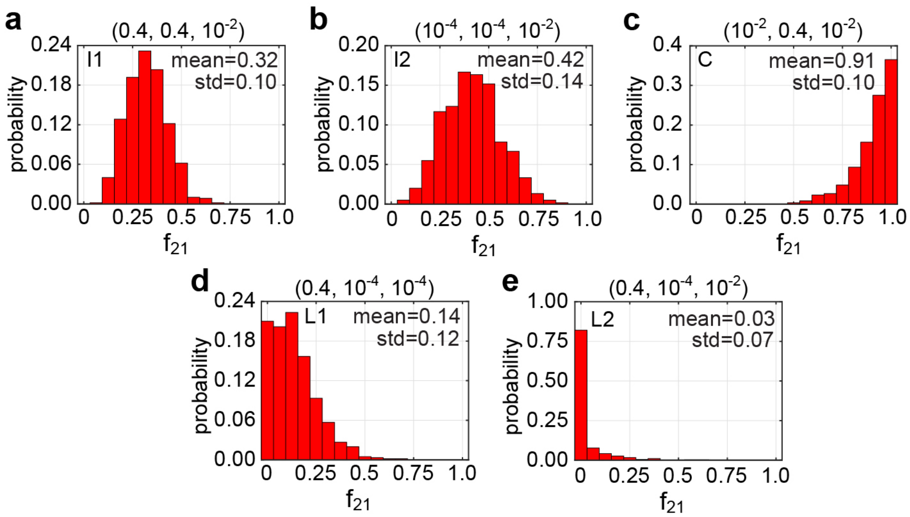

Fig. S13 Distribution of f_{21} for five representative structures shown in Fig. 1.

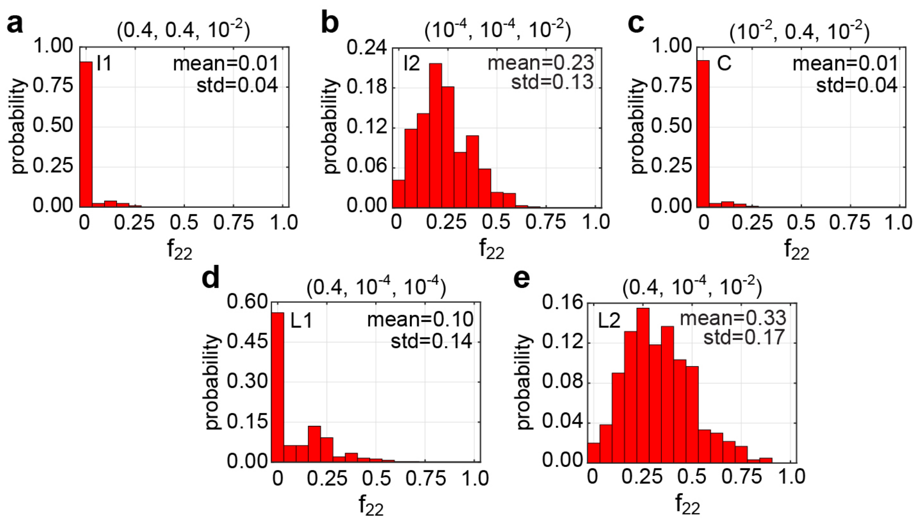

Fig. S14 Distribution of f_{22} for five representative structures shown in Fig. 1.

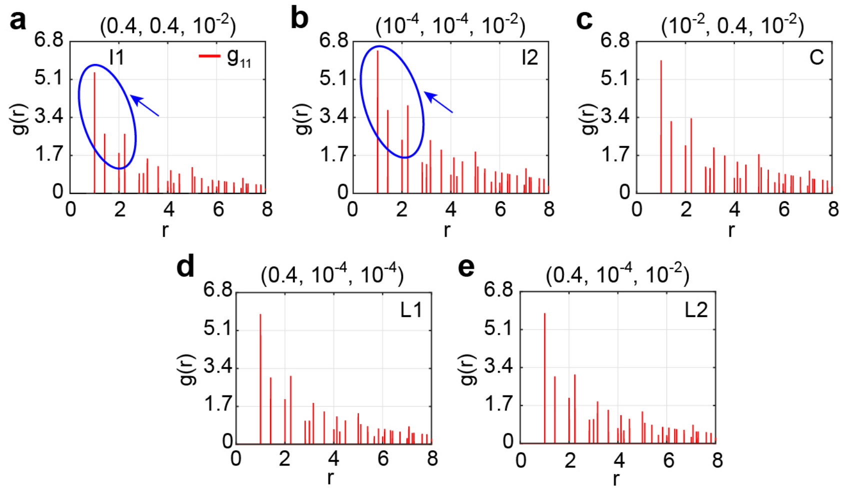

Fig. S15 Radial distribution function between NP1 particles. We fixed the number of NPs in the system at N_1=10000 and N_2=200. The sticking probabilities are specified as (p_{11}, p_{12}, p_{22}). The blue arrows show the first four peaks of g_{11}.

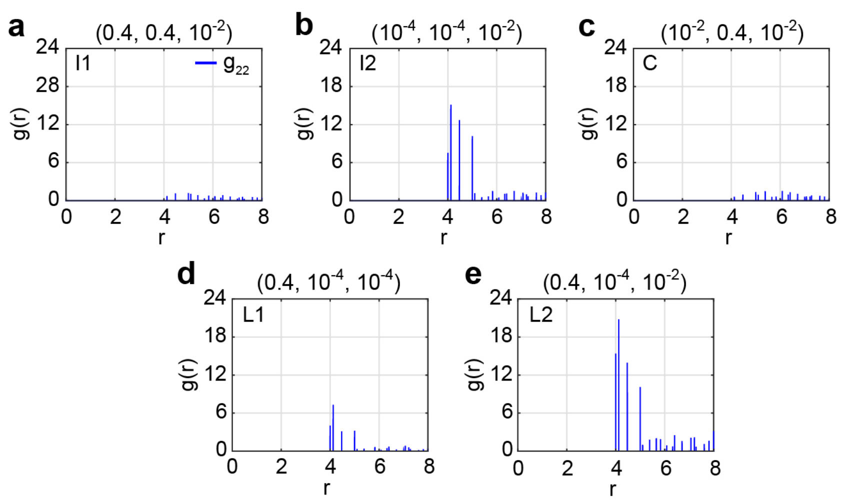

Fig. S16 Radial distribution function between NP2 particles. We fixed the number of NPs in the system at N_1=10000 and N_2=200. The sticking probabilities are specified as (p_{11}, p_{12}, p_{22}).

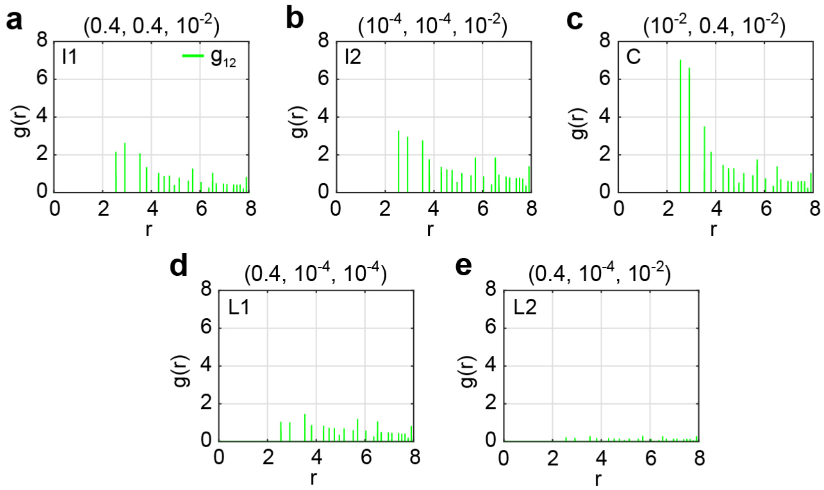

Fig. S17 Radial distribution function between NP1 and NP2 particles. We fixed the number of NPs in the system at N_1=10000 and N_2=200. The sticking probabilities are specified as (p_{11}, p_{12}, p_{22}).

5. Pore size of the aggregate structures

When we sample the pore size of the aggregate structures, the number of times that a pore of a certain size is sampled is proportional to the area of the pore. Therefore, the direct numerical average is taken as the area-average pore size. The number-average is calculated by $\bar{d} = \frac{\sum_{i=1}^{N_s} \frac{1}{d_i}}{\sum_{i=1}^{N_s} \frac{1}{{d_i}^2}}$, where N_s is the total number of samplings and d_i is the sampled pore size each time.

6. Structure factor

The structure factor can also be calculated by

$$S(q) = N^{-1} \sum_{i,j=1}^{N} \exp\left(-i \cdot q \cdot (\boldsymbol{r}_i - \boldsymbol{r}_j)\right), \quad \text{(s1)}$$

or

$$S(q) = N^{-1} \sum_{i,j=1}^{N} J_0(q|\boldsymbol{r}_i - \boldsymbol{r}_j|), \quad \text{(s2)}$$

where J_0 is the zero-order Bessel function of the first kind. As show in Fig. S16, structure factor obtained from different methods are consistent.

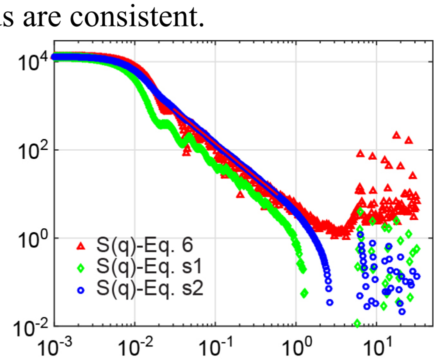

Fig. S18 Structure factor obtained from different methods when p_{11}=0.4, p_{12}=0.4, and p_{22}=0.01.

7. Phase diagram and representative aggregate structures with different morphologies

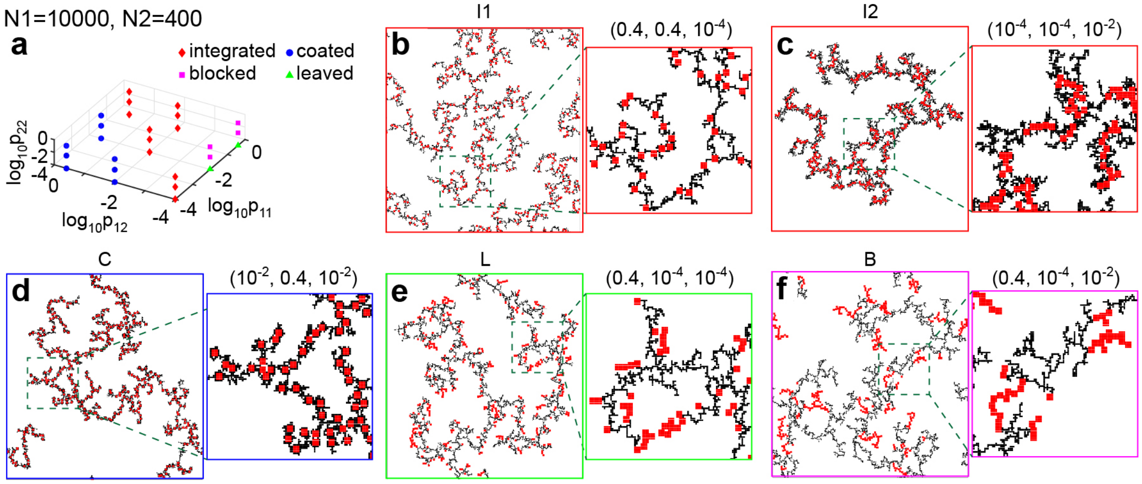

Fig. S19 Morphology phase diagram and representative aggregate structures of different morphologies obtained from simulations. We fixed the number of NPs in the system at N_1=10000 and N_2=400. The sticking probabilities are specified as (p_{11}, p_{12}, p_{22}).

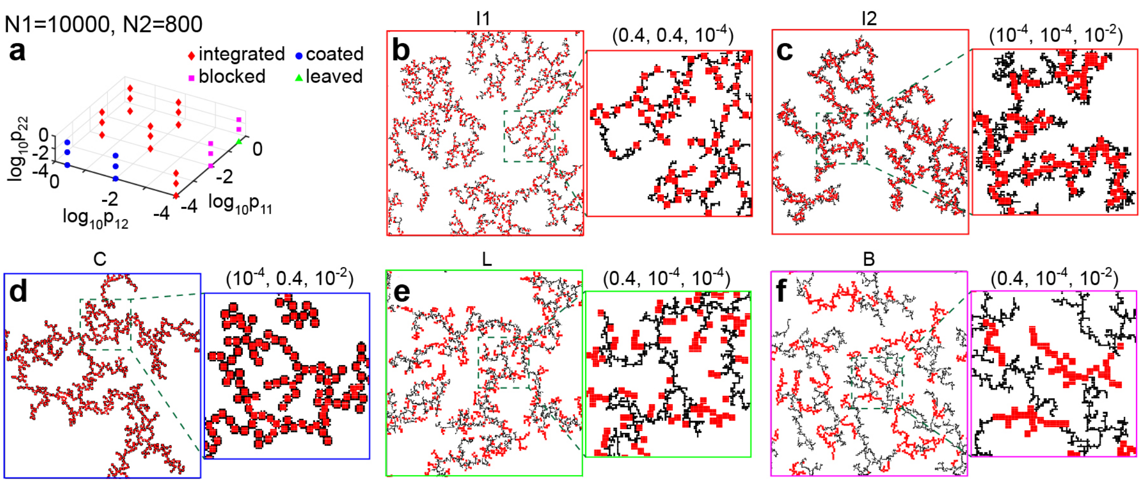

Fig. S20 Morphology phase diagram and representative aggregate structures of different morphologies obtained from simulations. We fixed the number of NPs in the system at N_1=10000 and N_2=800. The sticking probabilities are specified as (p_{11}, p_{12}, p_{22}).

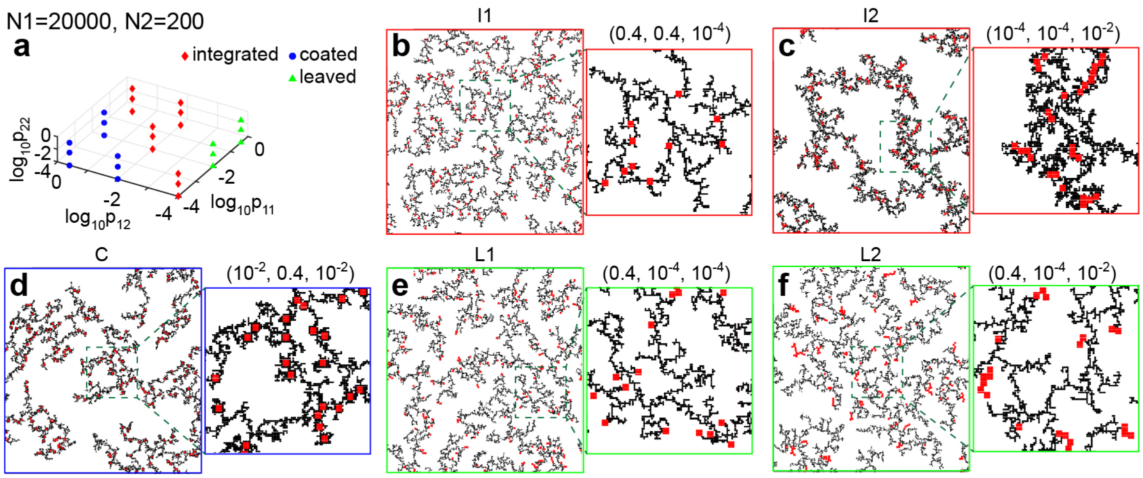

Fig. S21 Morphology phase diagram and representative aggregate structures of different morphologies obtained from simulations. We fixed the number of NPs in the system at N_1=20000 and N_2=200. The sticking probabilities are specified as (p_{11}, p_{12}, p_{22}).

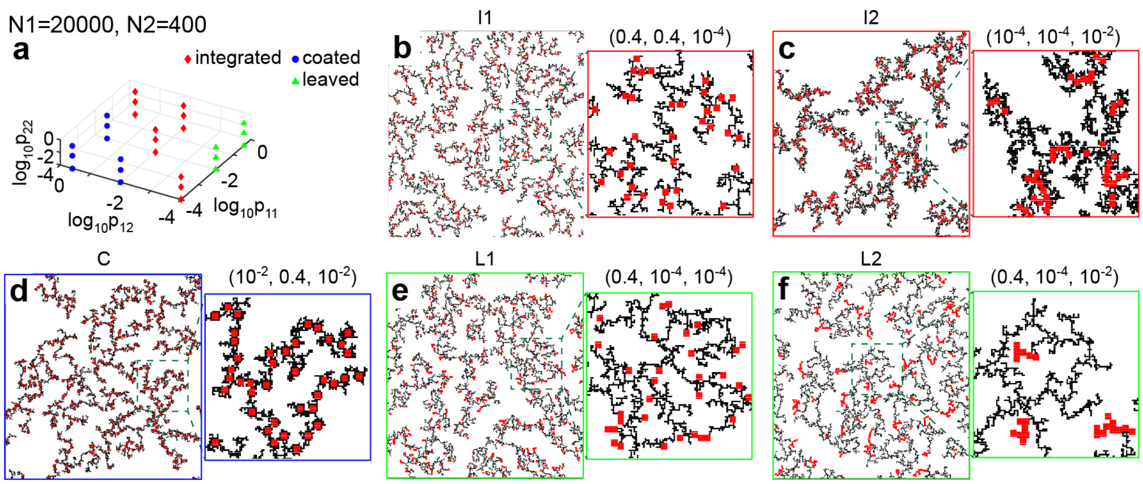

Fig. S22 Morphology phase diagram and representative aggregate structures of different morphologies obtained from simulations. We fixed the number of NPs in the system at N_1=20000 and N_2=400. The sticking probabilities are specified as (p_{11}, p_{12}, p_{22}).

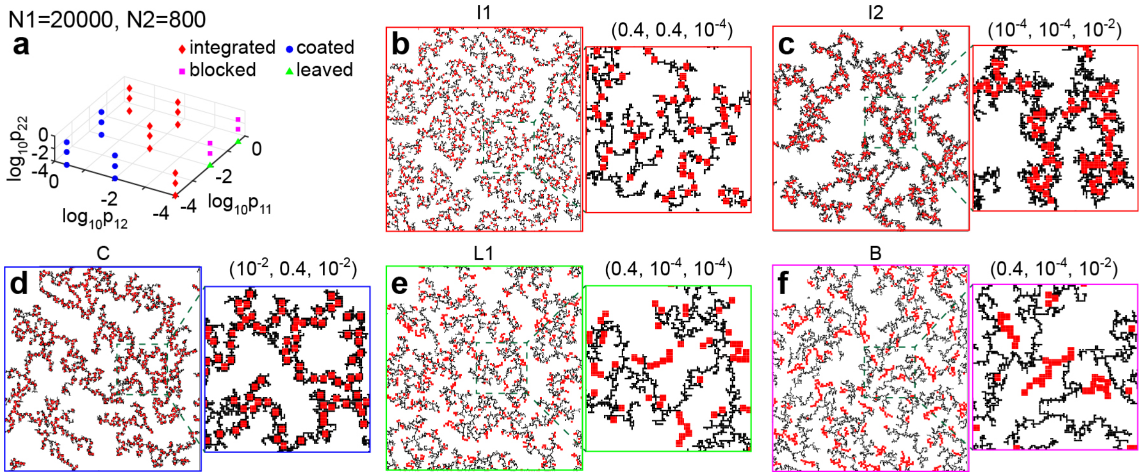

Fig. S23 Morphology phase diagram and representative aggregate structures of different morphologies obtained from simulations. We fixed the number of NPs in the system at N_1=20000 and N_2=800. The sticking probabilities are specified as (p_{11}, p_{12}, p_{22}).

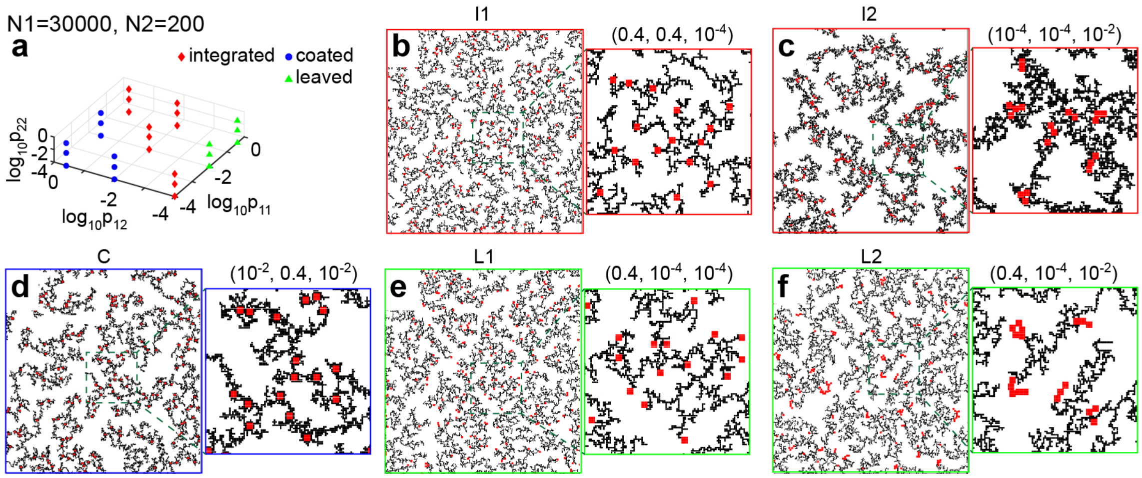

Fig. S24 Morphology phase diagram and representative aggregate structures of different morphologies obtained from simulations. We fixed the number of NPs in the system at N_1=30000 and N_2=200. The sticking probabilities are specified as (p_{11}, p_{12}, p_{22}).

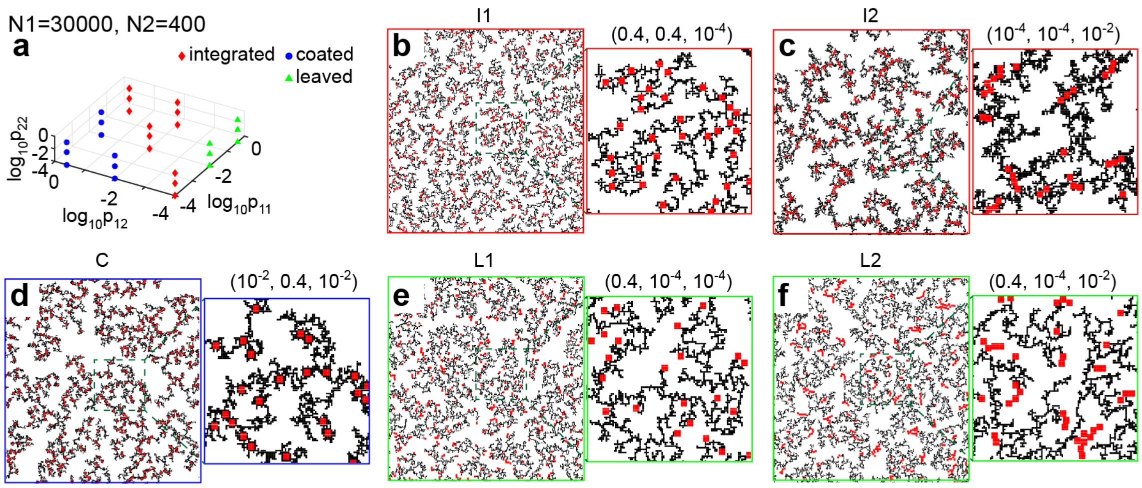

Fig. S25 Morphology phase diagram and representative aggregate structures of different morphologies obtained from simulations. We fixed the number of NPs in the system at N_1=30000 and N_2=400. The sticking probabilities are specified as (p_{11}, p_{12}, p_{22}).

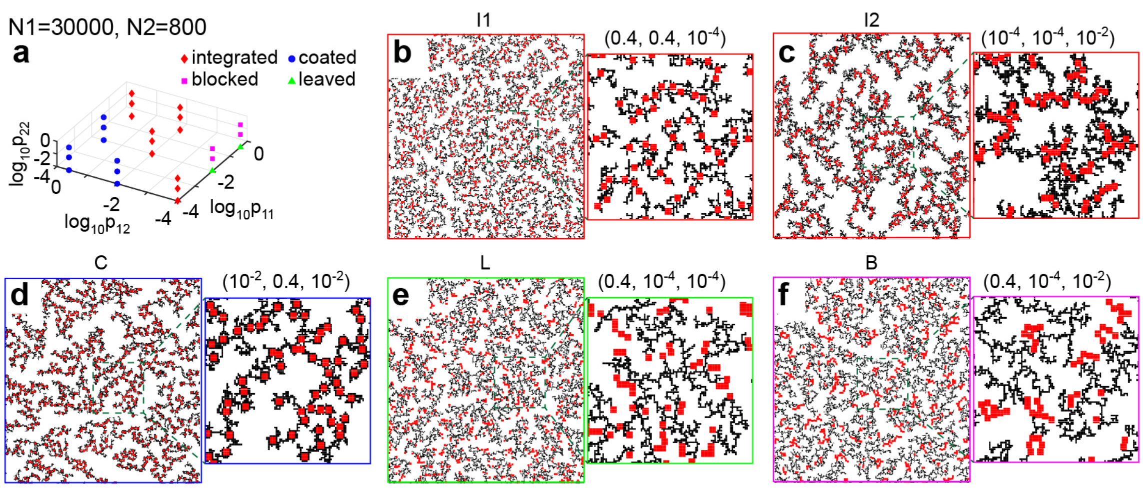

Fig. S26 Morphology phase diagram and representative aggregate structures of different morphologies obtained from simulations. We fixed the number of NPs in the system at N_1=30000 and N_2=800. The sticking probabilities are specified as (p_{11}, p_{12}, p_{22}).

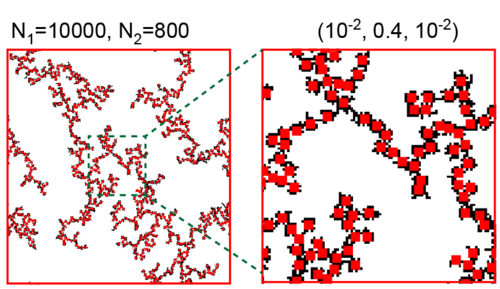

Fig. S27 Aggregate structures when N_1=10000, N_2=800, p_{11}=0.01, p_{12}=0.4 and p_{22}=0.01. Due to insufficient NP1 particles, the system forms an integrated phase rather than a coated phase.

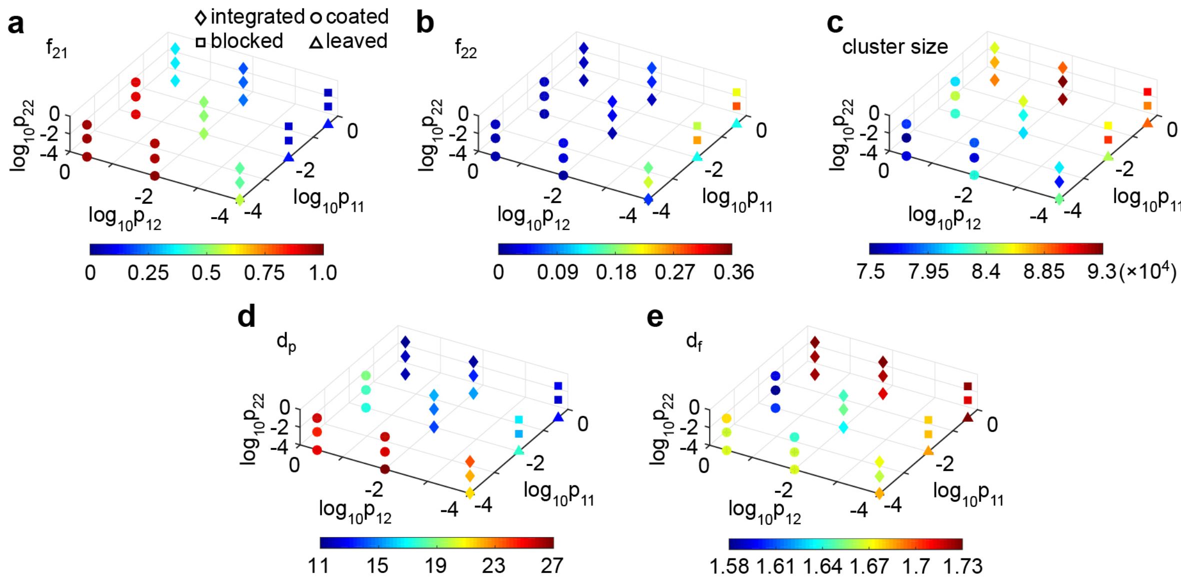

Fig. S28 Phase diagrams in local distribution, cluster size, fractal dimension, and porosity of aggregate structures as a function of sticking probabilities. We fixed the number of NPs in the system at N_1=30000 and N_2=800. (a) Average value of f_{21}. (b) Average value of f_{22}. (c) Cluster size of aggregates. (d) Area-average pore size of aggregates. (e) Fractal dimension d_f obtained from structure factor. These results are averaged over 15 independent simulation runs.

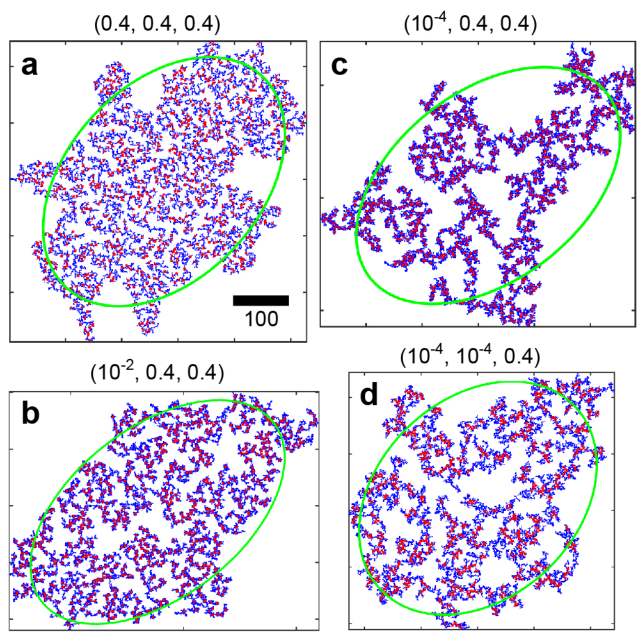

Fig. S29 Representative aggregate structures obtained with N_1=30000 and N_2=800. Sticking probabilities are specified in the figures.

Table S1 Fractal dimension, cluster size, and area-average pore size of aggregate structures obtained from the binary and unary NP systems. Values listed here correspond to those plotted in Figure 7.

Phase	Fractal dimension	Cluster size ($\times 10^4$)	Pore size
Integrated	1.52, 1.51, 1.50, 1.50, 1.53, 1.54, 1.52, 1.55, 1.55, 1.62, 1.62, 1.64	6.4, 6.1, 6.2, 6.0, 5.8, 5.6, 4.9, 5.0, 4.6, 3.7, 3.4, 3.8	38.0, 39.0, 43.2, 39.9, 38.3, 39.9, 38.4, 43.0, 35.8, 35.3, 31.0, 31.6
Coated	1.52, 1.54, 1.53, 1.59, 1.59, 1.61, 1.58, 1.59, 1.62	4.3, 4.7, 4.4, 3.6, 3.2, 3.2, 3.4, 3.3, 3.3	37.8, 43.5, 35.0, 32.2, 28.2, 31.6, 29.2, 30.1, 30.8
Leaved	1.53, 1.51, 1.56, 1.53, 1.56, 1.59	6.2, 5.8, 5.6, 4.7, 4.7, 4.4	39.4, 37.4, 34.8, 34.4, 36.6, 36.0
Unary assembly	1.53, 1.53, 1.54, 1.56, 1.62	6.4, 6.1, 5.1, 4.2, 3.9	35.8, 32.8, 36.2, 32.8, 32.3

7. Effect of simulation box size

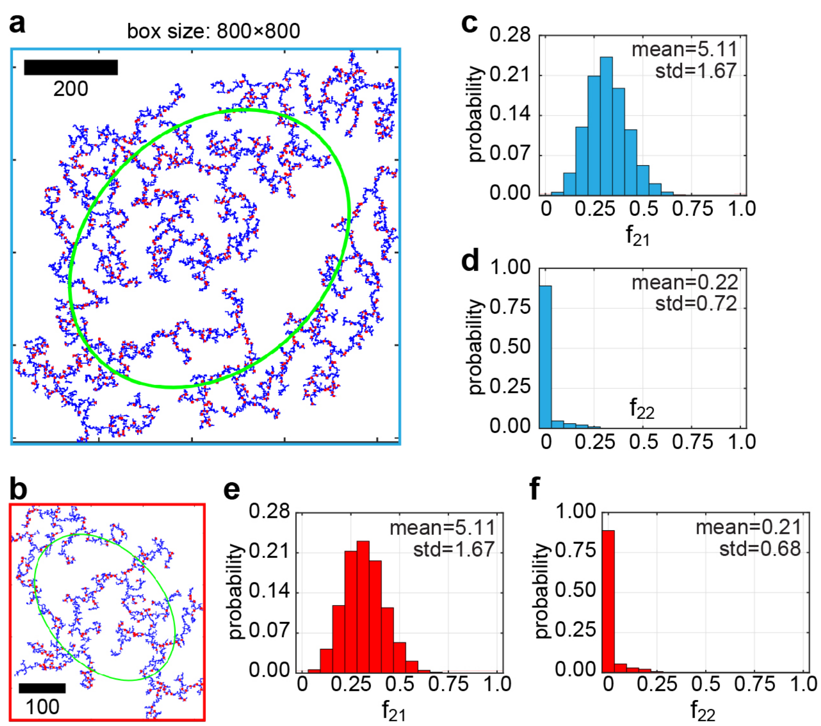

Fig. S30 Effect of simulation box size on the local distribution of particles in the formed binary NP aggregates. (a, b) Representative unwrapped structures of aggregates obtained from simulations conducted on a large 800×800 lattice (a) and the original 400×400 lattice (b). The number density of the two species of NPs was kept identical in both systems, specifically, N_1=40000, N_2=800 in (a) and N_1=10000, N_2=200 in (b), and the sticking probabilities were also set to the identical values, specifically $p_{11} = p_{12} = p_{22} = 0.4$, in both systems. (c, d) Distributions in f_{21} and f_{22} obtained from structures simulated on the 800×800 simulation box. (e, f) Distributions of f_{21} and f_{22} obtained with the smaller 400×400 box.

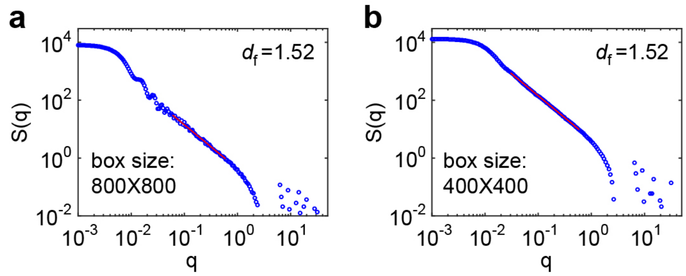

Fig. S31 Effect of simulation box size on the fractal dimension of aggregates. (a, b) Fractal dimensions obtained from structure factors when the box size is 800×800 (a) and 400×400 (b). Parameters used are the same as those stated in Fig. S30.